Looking and listening to light: the evolution of whole-body photonic imaging

Vasilis Ntziachristos[1], Jorge Ripoll[1,2], Lihong V Wang[3] & Ralph Weissleder[1]

Optical imaging of live animals has grown into an important tool in biomedical research as advances in photonic technology and reporter strategies have led to widespread exploration of biological processes *in vivo*. Although much attention has been paid to microscopy, macroscopic imaging has allowed small-animal imaging with larger fields of view (from several millimeters to several centimeters depending on implementation). Photographic methods have been the mainstay for fluorescence and bioluminescence macroscopy in whole animals, but emphasis is shifting to photonic methods that use tomographic principles to noninvasively image optical contrast at depths of several millimeters to centimeters with high sensitivity and sub-millimeter to millimeter resolution. Recent theoretical and instrumentation advances allow the use of large data sets and multiple projections and offer practical systems for quantitative, three-dimensional whole-body images. For photonic imaging to fully realize its potential, however, further progress will be needed in refining optical inversion methods and data acquisition techniques.

Small-animal imaging is rapidly becoming a cornerstone in biomedical investigation, serving as an important translation tool between *in vitro* research and clinical application. Recently, key advances in the *in vivo* reporting of genomics and proteomics have intensified the development of dedicated small-animal imaging systems and strategies[1–6]. Linked to these developments is an emerging shift from traditional *in vitro* assay–based research to *in vivo* imaging–based research. *In vivo* imaging can improve our ability to probe complex biologic interactions dynamically and to study disease and treatment responses over time in the same animal, thus offering the potential to accelerate basic research and drug discovery using fewer animals.

Two major approaches have been adopted in the development of *in vivo* small-animal imaging. The first is an elegant adaptation of proven clinical imaging technologies to the smaller animal dimensions. It includes all of the major radiological modalities; that is,

positron emission tomography (PET), single photon emission computed tomography (SPECT), magnetic resonance imaging (MRI), ultrasound, X-ray computed tomography (CT) and multi-modality approaches[1,5,6]. The resulting imaging systems attain higher resolution and detection sensitivity compared with their clinical counterparts because of the smaller field of view used and the corresponding modification of the operating characteristics (for example, higher field strengths for MRI or higher frequencies for ultrasound).

The second approach focuses on new imaging technologies, primarily macroscopic imaging based on photonics. These novel methods extend beyond three-dimensional *in vivo* microscopy (such as multi-photon or confocal microscopy), which is not well suited for whole-body imaging because of its limited penetration depth (<1 mm) and the restricted field of view typically achieved. Here, progress in instrumentation and methodology is combined with ingenious advances in fluorescence or bioluminescence reporter gene/reporter probe[1,4,7] strategies, activatable fluorescent probes and targeted fluorescent probes[8,9] for *in vivo* molecular sensing. Whole-body fluorescence and bioluminescence imaging have transformed the ways gene expression and protein functions are visualized *in vivo*[10,11]. In most cases, optical detection has been accomplished using photographic methods, using low-light cameras and appropriate filters. Photon attenuation, however, is strongly nonlinear as a function of depth and of the optical heterogeneity of tissue, which obscures signal quantification. Planar imaging is further complicated by the inability to resolve depth and by tissue scattering, which limits spatial resolution. For these reasons, although planar methods are useful, they do not harness the true potential of the optical imaging technologies.

The emergence of mathematical models that describe photon propagation in tissues, combined with advanced illumination and detection schemes, and appropriate tomographic principles, can significantly improve visualization capacity in tissue. Tomography enables quantitative three-dimensional volumetric imaging of opaque media and can overcome planar imaging limitations. The combination of these advances with adept contrast mechanisms using highly specific fluorescent probes or the photoacoustic phenomenon has facilitated a new generation of photonic imaging systems that is rapidly maturing and can greatly facilitate small-animal research by complementing the laboratory microscope, spectrophotometer and flow cytometer with whole-body *in vivo* molecular imaging capacity.

This review focuses on novel macroscopic photonic imaging technologies that, in combination with emerging reporter strategies, promise to provide researchers with unprecedented power to visualize biological processes. We compare photographic and tomographic optical imaging and describe the three major optical domains of optical tomography

[1]Center for Molecular Imaging Research (CMIR), Massachusetts General Hospital & Harvard Medical School CNY149, 13th street 5406, Charlestown, Massachusetts 02129, USA. [2]Institute for Electronic Structure and Laser, Foundation of Research and Technology-Hellas, P.O. Box 1527, 71110 Heraklion, Greece. [3]Optical Imaging Laboratory, Department of Biomedical Engineering, Texas A&M University, 3120 TAMU, College Station, Texas 77843-3120, USA. Correspondence should be addressed to V.N. (vasilis@helix.mgh.harvard.edu).

a Reflectance

b Transillumination

Input
Output

Input
Output

Diffusive photons

c Tomography

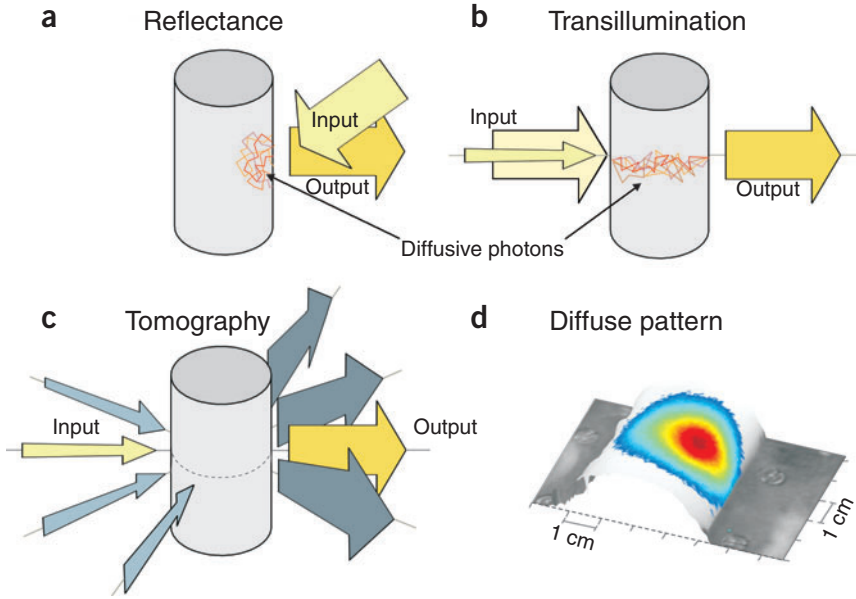**d** Diffuse pattern

Input
Output

1 cm
1 cm

Figure 1 Modes of data collection. (**a**,**b**) Planar imaging. Fluorescence reflectance imaging. Excitation light (input) is expanded on the object surface and fluorescence light (output) collected from the same side of the object. Scattered photon trajectories are simplistically demonstrated with a few lines to demonstrate the typical volume sampling. (**b**) Transillumination illuminates the object from the opposite side from the data collection so that light propagates through the object. Photon scattering is also indicated with a few lines and indicates the volume sampling differences in relation to **a**. Transillumination can be obtained with a single point source (green), a summation of multiple point sources or with an expanded planar beam (light gray). (**c**) Tomography. Illustration of data collection where multiple point-source transillumination data are time-shared around a cylindrical geometry. Different geometries and the use of reflected data can also be used for tomographic purposes. The direction indicated by the arrows shows the general photon trajectory established. The pattern of data collected is, in fact, diffusive as is evident from the experimental measurements shown in (**d**) obtained from a transilluminated homogeneous diffusive cylinder.

(that is, time, frequency and constant intensity). Particular weight is given to recent noncontact imaging approaches and tomographic specifics that significantly improve imaging performance and enable the development of practical and accurate systems. State-of-the-art *in vivo* imaging examples are illustrated. Bioluminescence and photoacoustic tomography are also reviewed, together with the expected impact of these technologies in biomedical research.

Planar imaging
Planar imaging, the simplest technique for detecting optical reporter molecules *in vivo,* uses photographic principles to capture light emitted from the animals[12–14] and has broadly affected biomedical research[7,11,15]. For fluorescence imaging, the animal is typically illuminated with a broad light beam tuned to the excitation wavelength of the fluorochrome of interest and is photographed at the emission wavelengths by a highly sensitive and low noise charged-coupled device (CCD) camera using appropriate filters and large aperture lenses for high photon collection efficiency (**Fig. 1a**). These low-light images are superimposed on mouse photographs obtained at the excitation wavelength or with white light illumination. This is the most common whole-body fluorescence imaging approach today and is termed fluorescence reflectance imaging (FRI). Advanced forms of FRI use spectral information to differentiate between different fluorochromes. Yang *et al.*[14], for example, demonstrated that the use of a highly sensitive color CCD camera can detect green fluorescent proteins expressed

by tumors implanted superficially in living animals. More recently, to improve detection contrast (see **Fig. 2**), Gao *et al.*[16] have used spectral un-mixing, a technique that can differentiate multiple fluorochromes from nonspecific background fluorescence on the basis of their spectral characteristics (for details, see ref. 17). Bioluminescence signals can be similarly detected, but in the absence of external illumination light. In contrast, fluorescence transillumination imaging illuminates the animal with a broad light beam or a raster scan of focused beam and images are collected from the opposite side of the illumination source (**Fig. 1b**).

Planar imaging offers an attractive tool for high-throughput imaging and it is technically easy to implement. However, it also has important limitations, such as the single projection viewing, the restricted penetration depth of a few millimeters and the nonlinear relationship between the signal strength and the depth and the tissue optical properties. These features limit the applicability of the method primarily to superficial observations and may lead to erroneous interpretation of the data collected if the nonlinear effects are not explicitly corrected or accounted for. **Box 1** outlines some examples of planar imaging limitations in relation to depth and tissue optical properties and contrasts them with tomography.

Fluorescence tomography
Tomographic reconstruction of fluorescence biodistribution has its roots in the early 1990s when the first theoretical frameworks for tomography of diffuse media were proposed to spatially resolve intrinsic tissue contrast (primarily absorption and scattering) in the
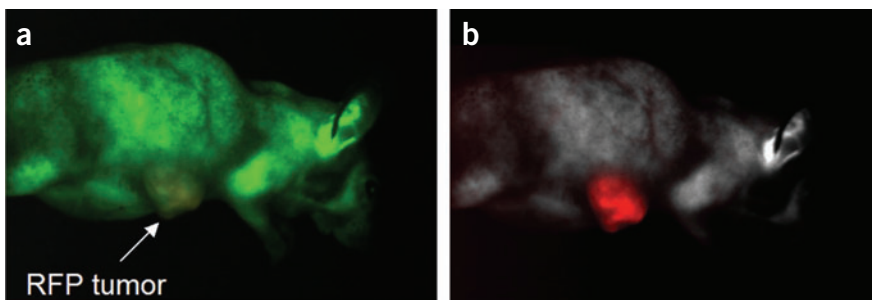
a

RFP tumor

b

Figure 2 Spectral imaging applied to *in vivo* fluorescence detection. (**a**) Standard color image obtained from a green fluorescence protein (GFP)-expressing mouse implanted with a red fluorescent protein (RFP)-expressing tumor. (**b**) Spectral imaging and processing improves visualization of the RFP signal, which can be separated from the mouse intrinsic auto-fluorescence and GFP fluorescence. Images and analysis were provided by Cambridge Research & Instrumentation (CRI); samples were provided by Anticancer.

context of studying hemodynamics or organelle concentration[18–21]. This work followed original observations that near-infrared light (NIR: 650 nm–900 nm) can penetrate several centimeters into tissues because of the low photon absorption in this spectral window[22,23]. In contrast to high-energy rays, however, NIR photons are highly scattered in tissue and they become diffuse within approximately a millimeter of propagation[24]. For tomography, multiple points on the tissue boundary are illuminated in a time-sharing fashion (**Fig. 1c**) and diffuse light patterns are collected around the boundary (**Fig. 1d**) using photodetector sets or a CCD camera. Each source-detector pair effectively implements a different projection through the tissue,

albeit following diffusive propagation patterns . Fluorescence measurements can be obtained using appropriate filters in front of the detectors, although the same generic tomographic principles are used for reconstruction of intrinsic tissue contrast, that is, absorption or scattering. These measurements are then combined in a tomographic scheme, which can be written as a system of equations that are solved for the unknown, spatially dependent fluorochrome concentration. This generic mainframe, combined with appropriate fluorescent molecules with specificity to cellular and sub-cellular processes, has led to the development of fluorescence molecular tomography (FMT), a technology directed towards noninvasive quantitative

Box 1 Performance characteristics of planar and tomographic imaging

A side-by-side comparison of the performance of planar and tomographic imaging in visualizing tissue-mimicking phantoms reveals some of the likely drawbacks of the former approach in imaging small animals. **Figure 6a** shows planar and tomographic imaging of two ~1.5-mm diameter fluorescent tubes containing cyanine 5.5, which are immersed in a diffusive fluid with the average optical properties of small animals and imaged through a glass window. Both planar and FMT resolve the tubes when they are placed in contact with the glass window, although FMT offers better resolution. However, planar imaging detection becomes highly challenging as the tubes move deeper in the diffuse medium, away from the glass window, even at the 3 mm depth. Depth sensitivity depends strongly on the light strength used and the size and concentration of the fluorochrome used, but the images demonstrate the superior ability of tomography to look deeper into diffuse media with higher resolution, using in this case identical hardware to that used with the planar imaging. The color images are reconstructed slices obtained at different depths and superimposed on gray scale photographs of the tubes for visualization purposes[52].

Similarly, imaging fluorochromes with varying background optical properties is shown in **Figure 6b**. Both planar and FMT accurately resolve the 2:1 relation in fluorochrome concentration between the left and right tubes when the background absorption is the same in both tubes (top row). However, when India ink is added in the left tube to simulate a threefold increase in vascularization (absorption), the planar image erroneously reports a ~1:1 cyanine 5.5 concentration in the two tubes (bottom row). This is because the added ink absorbs more fluorescent photons. In contrast, FMT can correct for the added absorption and demonstrates more robust performance, reporting 1.8:1 relation in this case[52].

Finally, **Figure 6c** demonstrates the capacity of FMT to image fluorochromes in a highly diffusive medium that simulates tissue optical heterogeneity. The image labeled nBorn shows that the use of normalization methods (in this case, as described in ref. 41) can accurately resolve the fluorescence distribution, despite the highly heterogeneous background. The absence of data normalization, however, yields images that are affected by the background heterogeneity, as shown in the image labeled hBorn. The planar imaging could not detect the presence of the fluorochrome in this case.

Overall, these findings indicate that planar imaging should be used with caution. Signal intensity relates linearly to fluorochrome concentration but nonlinearly to depth, size and optical properties, and its measurement is further complicated by the highly scattering nature of tissue. FMT has the potential to circumvent some of these limitations and offers more robust and accurate imaging.
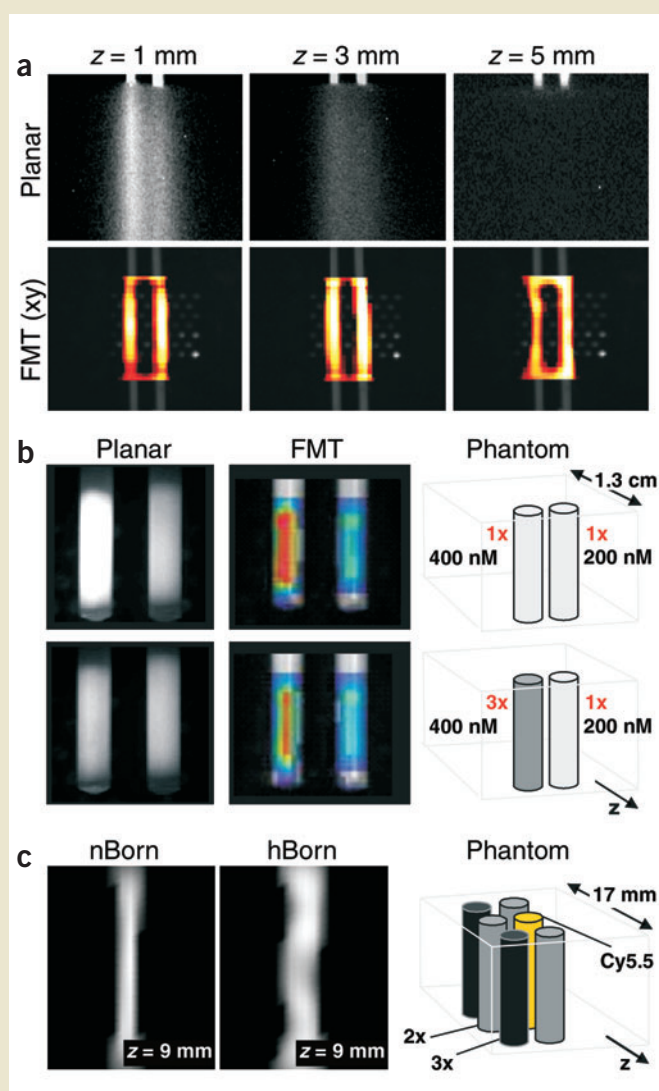

Figure 6 Performance of planar and tomographic imaging. (**a**) Two ~1.5mm diameter fluorescent tubes (500 nM cyanine 5.5, 3 mm apart) immersed at different depths in an intralipid and India ink solution, simulating the optical properties of small animals. (**b**) Planar and reconstructed images of two fluorescent tubes, the left containing twice as much cyanine 5.5 as the right tube (400 nM versus 200 nM). The tubes are immersed in the same diffuse fluid as in **a**. (**c**) A single fluorescing tube is asymmetrically surrounded by five absorbers at twofold and threefold the background absorption. The tube is reconstructed using a normalized (nBorn) and not normalized method (hBorn).

Table 1 Optical domains

Domain	Time	Frequency	Continuous wave
Resolution[a]	0.5–1 mm	0.5–1 mm	1 mm
Sensitivity[a]	Picomoles	Picomoles	Picomoles-femtomoles
Depth[b]	<30 mm	<30 mm	<50 mm
Contrast	T, A/S, F/L	T, A/S, F/L	T, F, B
Fluorochrome quantification	Yes	Yes	Yes
Signal-to-Noise Ratio	Medium	Medium	High
Cost	High	Medium/high	Low/medium

[a]Reported for fluorochromes at the center of 15 mm thick tissues. [b]Assuming ~10 picomoles of an organic fluorochrome.
A, absorption; S, scattering; F, fluorescence concentration; L, fluorescence lifetime; T, attenuation, B, bioluminescence.

molecular imaging of whole animals and tissues. Tomography can overcome several of the limitations of planar imaging, as summarized in **Box 1**.

Optical domains. There are three distinct illumination-detection technology domains for optical tomography; that is, the time-domain (TD), the frequency domain (FD) and the continuous wave (CW) domain. Each has distinct advantages and disadvantages, and the selection of the appropriate technology largely depends on the specific application (**Table 1**).

For molecular investigations where the goal is to localize and quantify fluorescent probes, CW imaging offers excellent detection characteristics. CW domain methods use light of constant intensity and require simple and low-cost optical components[25]. They further offer optimum signal-to-noise performance because CW light sources and detectors are typically more stable and have low noise characteristics compared with those sources and detectors used in TD and FD methods. The major disadvantages of CW domain methods include the difficulty of resolving the tissue absorption from scattering and the inability to image fluorescence lifetime. Another caveat is that, unlike TD or FD methods, resolution is entirely dependent on a tissue's optical properties and geometry; it can not otherwise be optimized.

When independent measurements of tissue absorption, scattering or fluorochrome lifetime are required, the use of TD or FD technology becomes essential[22,26,27]. TD methods illuminate tissue with ultrafast (femtosecond to picosecond) photon pulses and resolve the arrival of the photons as a function of time at different locations around the tissue boundary. In contrast to CW methods, they can use early arriving photons to improve resolution because highly diffusive photons are rejected[28–30]. On the downside, TD methods are less sensitive than CW methods because of the lower duty cycles achieved (that is, the length of time the laser beam and detector is on), resulting in dimmer average light intensity available for imaging. In addition, TD instrumentation is noisier than CW systems due to time and intensity fluctuations that are associated with ultrafast switching electronics and pulsing lasers.

The third mode, FD technology, uses light of a modulated intensity at a frequency f, which establishes a photon wave of the same frequency in the diffuse medium[31]. Measurements of the light intensity and the phase shift of the photon wavefront away from the source or the excited fluorochromes reveal information about the tissue optical properties and fluorochrome bio-distribution[32]. FD methods are less affected by ambient light than CW and TD methods. However, they require frequencies of several hundred MHz or higher to achieve improvements in resolution over CW. They are also less robust than CW methods because of the reduced signal-to-noise detection involved in sensing high frequencies. Data obtained at multiple frequencies improve FD imaging performance and can become equivalent to TD data via the inverse Fourier Transform.

Improving spatial sampling. Previous fluorescence tomography investigations focused primarily on feasibility studies with simple tissue-mimicking phantoms and on algorithmic validation. Typical systems used a limited number of sources and detectors arranged around the tissue boundary using light-guiding fibers. In several instances, a matching fluid was used to surround the tissue and achieve optimal photon coupling and a simplified experimental arrangement; otherwise, fibers were brought in contact with the tissue. This technology typically yielded coarse spatial photon-sampling on the boundary, resulting in 10^2–10^3 total measurements, which is generally insufficient for high-fidelity volumetric imaging. In addition, the fiber-based technology complicated experimental procedures because either the tissue had to be surrounded by fluids or meticulous engineering had to be exercised to ensure the optimal contact of each individual fiber with the tissue[33]. This set of approaches compromised imaging performance and reduced overall enthusiasm for optical tomography.

More recently, it has been shown that submillimeter spaced arrays of sources and detectors (that is, data sets on the order of 10^4–10^6 measurements or more) are necessary for high-fidelity, small-animal imaging[25]. To achieve such large data sets, researchers have
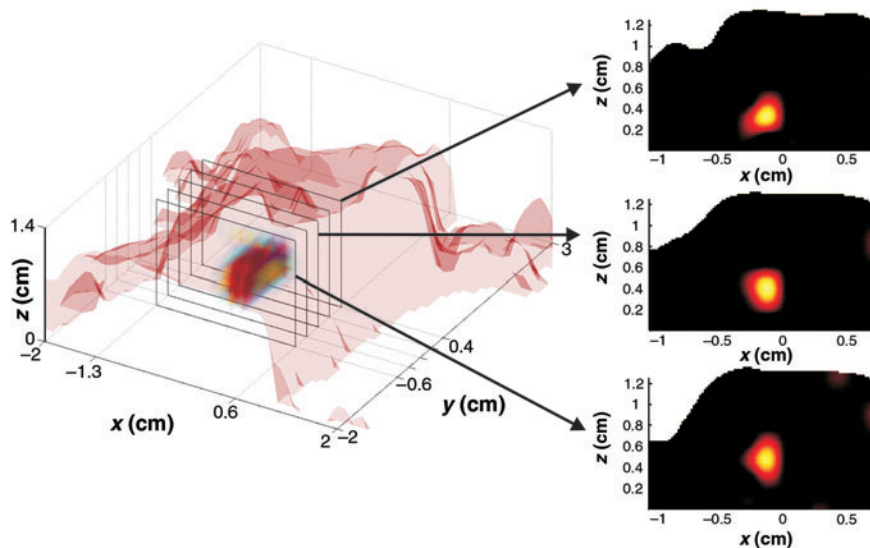

Figure 3 Fluorescence reconstruction of a fluorescent tube inserted in a euthanized animal obtained in the absence of contact detection. Image reconstruction is based on mathematical models that describe the composite photon propagation in tissue and in air (for details see ref. 36). The animal surface was captured using photo-grammetry, that is, the mathematical combination of photographs obtained under different angles to deduce the physical dimension of the animal.
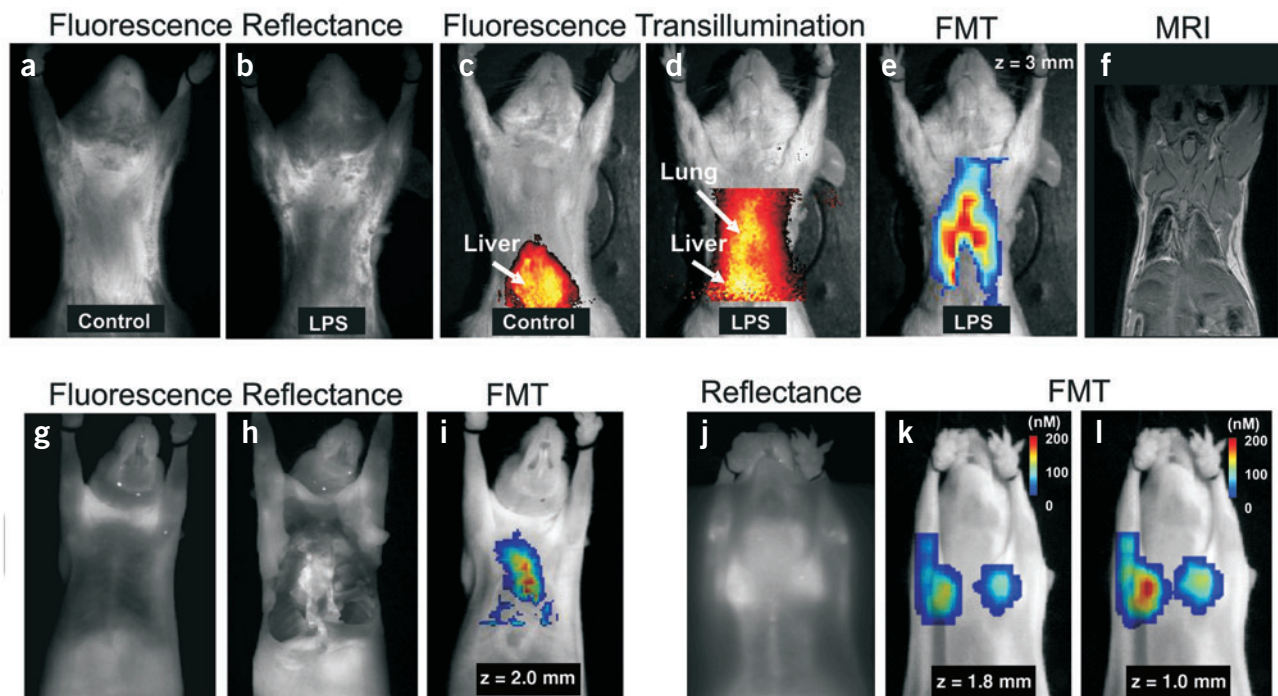
Figure 4 *In vivo* fluorescence imaging. (**a**–**e**) Imaging of proteolytic activity in LPS-induced pulmonary inflammation. Fluorescence reflectance images of the LPS-challenged and nonchallenged mouse (control) injected with a cathepsin-sensitive fluorescent probe (**a**,**b**). Fluorescence transillumination images of control and LPS-challenged mouse, respectively (**c**,**d**). Fluorescence Molecular Tomography slice (**e**) and corresponding T1-weighted MR image (**f**). (**g**–**i**) Imaging of lung tumors. *In vivo* fluorescence reflectance image (**g**). *Post mortem* fluorescence reflectance image after skin and rib-cage removal (**h**). (**i**) FMT slice at 2 mm depth under the surface. (**a**–**i**) Images are courtesy of investigators at the Laboratory for Bio-optics and Molecular Imaging/CMIR. (**j**–**l**) Differential imaging of treatment effects using an annexin V-Cy5.5 probe. *In vivo* planar reflectance image (**j**), two consecutive FMT slices obtained at 1 mm and 1.8 mm under the animal surface (**k**,**l**) (see text for details).

introduced free-space and noncontact imaging approaches. Free-space tomography is based on appropriate forward models that predict the composite propagation of photons in diffuse media and in air[34] and is enabled by noncontact collection methods, such as direct lens coupling of CCD cameras onto nonbounded tissue[35]. Free-space imaging is further combined with surface capture optical methods to yield an accurate description of the arbitrary tissue boundaries. These collection schemes offer high-quality data sets, high-spatial photon sampling and experimental simplicity because they both avoid the use of matching fluids/complex fiber interfaces and eliminate the associated fiber-tissue coupling issues. The feasibility of this approach has been recently showcased with phantoms[35] and animals[36]. **Figure 3** depicts reconstructed images of a 1.5-mm diameter fluorescent tube (500 nM of cyanine 5.5) inserted through the esophagus of a euthanized animal. With these advances, it is now possible to obtain practical, complete projection (360°), noncontact systems that, similar to other tomographic modalities (e.g., X-ray CT), can offer optimum imaging performance.

Forward problem and inversion. Two factors have a significant influence on tomographic performance: first, the selection of appropriate mathematical models that describe photon propagation in tissues (that is, the forward problem); and second, the selection of image reconstruction algorithms (that is, the inverse problem). Typical forward problems used for fluorescence tomography of tissues are based on numerical or analytical solutions of the diffusion equation[37–41] solved for the excitation and fluorescence fields. Forward models based on approximate solutions to the radiative transport equation[42] or on diffusion equation solutions merged with radiosity principles[43] have been proposed for

regimes where solutions of the diffusion equation become less accurate (such as, situations using early photons, millimeter-sized, source-detector separations or in void, nondiffusive regions).

A particular scheme that recently enabled *in vivo* application[44] has been the inversion of normalized data (that is, by solving for the ratio of fluorescence measurements over excitation measurements to minimize the sensitivity to tissue heterogeneity and to theoretical inaccuracies[41] (see **Box 1**). Such methods are computationally fast, robust and simple to implement and can be used with analytical and numerical solvers. More integrated approaches are based on iterative numerical solutions, and they handle heterogeneity explicitly by solving first for the background absorption and scattering and then implementing this information for fluorescence solutions[40]. Overall, the need for fast forward and inversion algorithms is becoming ever more important as data sets increase in size as a result of the application of newer generation noncontact instruments. The use of fast analytical solvers[45] or the acceleration of numerical solutions using, for example, multi-grid methods[46,47] are important contributions to achieving practical inversion schemes.

***In vivo* applications. Figure 4** summarizes FMT studies from our group using noncontact approaches for fluorescence tomography of small animals. The results are contrasted with planar imaging methods to illuminate differences. **Figure 4a–f** depicts findings from an *in vivo* imaging study of inflammatory lung disease. In this study, pulmonary inflammation was induced by intratracheal lipopolysaccharide (LPS) instillation in a BALB/c mouse using a previously described procedure[48] (LPS administration has previously been shown to upregulate cathepsins in macrophages as well as other pro-inflammatory pathways[49,50]). The

animal was imaged 24 h after challenge following administration of a fluorescence-activatable probe sensitive to major cathepsins (B > S, K, L) associated with inflammation[51]. Although the fluorescence reflectance images, shown in **Figure 4a,b**, are unable to resolve protease activity from the lung, transillumination images (**Fig. 4c,d**) do depict a marked difference in fluorescence distribution between the control and the LPS-treated animal. Correspondingly, a tomographic slice (**Fig. 4e**), obtained 3 mm under the surface, better demarcates the lung inflammation and demonstrates good congruence with the anatomical magnetic resonance image shown in **Fig. 4f**, which was obtained under identical placement conditions. **Fig. 4e** does not depict signal from the liver because the reconstruction algorithm automatically rejects fluorescence signals corresponding to excitation patterns that have been highly absorbed.

In a related example from our laboratory, a Lewis Lung carcinoma tumor (LLC), was grown in the lung of a nu/nu female after direct injection of 10[6] LLC cells mixed with MatrigelHC and targeted with the same fluorescent activatable probe used in **Fig. 4a–e**. The tumor was not visible on fluorescence reflectance images (**Fig. 4g**) *in vivo* but could be seen by FRI when the skin and the front rib cage were removed after the mouse was killed (**Fig. 4h**). Conversely, FMT (**Fig. 4i**) could detect contrast congruent with the appearance of the tumor. Tomographic feasibility to resolve molecular activity in animal brain tumors has also been shown based on fiber-based systems[44].

Finally, in **Figure 4j–l**, we illustrate the ability of tomography to image treatment effects *in vivo*. In this study[52], a mouse bearing LLC tumors sensitive and resistant to cyclophosphamide was treated with the drug and injected with a phosphatidylserine (PS)-sensing annexin V–based probe conjugated to the cyanine 5.5 fluorochrome to probe apoptosis. In **Figure 4j–l**, the drug-sensitive and drug-resistant tumors are in the left and right mammary area, respectively. Because of the superficial nature of the tumors, both the planar (**Fig. 4j**) and the two tomographic slices obtained from two adjacent depths (**Fig. 4k,l**) resolve the tumors. The tomography, however, allows more accurate quantification, tumor-to-tissue contrast, depth and size estimation. Planar imaging did not correctly indicate levels of apoptosis in some instances because of unequal absorption between the two tumors[52].

Bioluminescence tomography

Bioluminescence imaging uses enzymes, which convert unique substrates into light in the presence of oxygen and other factors (e.g., ATP, Mg)[4]. The propagation of emitted photons can be modeled, similarly to fluorescence photon propagation, as a diffusion process. Bioluminescence tomography can therefore be based on the same framework used for fluorescence tomography but light is collected from the subject in the absence of external illumination sources. Because internal bioluminescent light is continuously on during the measurement, bioluminescence tomography operates only in CW mode. One of the major advantages of the technique is that there is no inherent background bioluminescence in most tissues, which yields high imaging contrast. Methods for bioluminescence tomography have recently been reported[53,54], and there is a great impetus for *in vivo* tomographic applications for improving localization and quantification beyond what has been achieved by planar methods.
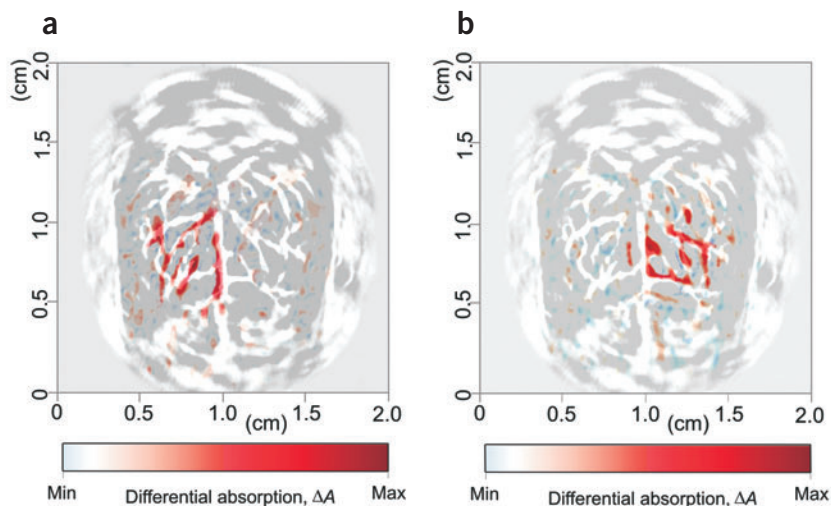

Figure 5 Visualization of brain structure and function using photoacoustic tomography (modified from ref. 57. (**a**,**b**) Functional maps of brain activities corresponding to the left-side (**a**) and right-side (**b**) whisker stimulations, respectively, acquired with the skin and skull intact.

However, the unavailability of external illumination sources complicates the tomographic problem, compared to fluorescence tomography, because it becomes mathematically more difficult and possibly less accurate, to resolve problems of internal sources (bioluminescence) compared with problems using external sources (fluorescence) because of the fewer source-detector pairs (projections) available. This problem is also common in other tomography methods (e.g., SPECT versus CT), although the experimental and image formation characteristics are different for high-energy and near-infrared photons. A combination of multi-view angle (360°) imaging with a priori information on tissue heterogeneity could improve the performance of the bioluminescence inverse problem[53]. *In vivo* applications of bioluminescence tomography have not yet been reported; however this technology is being actively researched and may become available in the future.

Photoacoustic tomography

When a short laser pulse, typically in the nanosecond range, is spatially broadened and then used to irradiate biological tissue, it produces a temperature rise on the order of milli-Kelvin in a short time frame. Consequently, thermoelastic expansion causes emission of acoustic waves, referred to as photoacoustic waves, that can be measured by wideband ultrasonic transducers around the sample. This phenomenon, discovered by Alexander Graham Bell, has been recently exploited for small-animal imaging, because the acquired photoacoustic waves can be combined mathematically to reconstruct the distribution of optical energy absorption[55,56]. The technique, termed photoacoustic tomography (PAT), also referred to as opto-acoustic or thermoacoustic tomography, attains the advantage of combining ultrasonic-scale spatial resolution with high sensitivity to tissue light absorption[57,58] and can yield information on physiology or on exogenously administered light absorbers.

This technique has been used recently for visualization of the brain structure and lesions, of cerebral hemodynamic responses to hyperoxia and hypoxia and of cerebral cortical responses to neuroactivities induced by whisker stimulations in rats[57]. **Figure 5** depicts two images of the superficial cerebral cortex of the rat after stimulation of the left-side and the right-side rat whiskers, respectively. These

images were obtained after subtraction of the image without whisker stimulations from the two PAT images with whisker stimulations. This differential contrast is attributed to the altered blood volume and oxygenation associated with the whisker stimulations. Similarly, noninvasive *in vivo* imaging of exogenous contrast agents in the rat brain using indocyanine green stabilized with polyethylene glycol has been also demonstrated[56].

Outlook

The advancement of new whole-animal imaging technologies presents new opportunities for biomedical research. Tomographic methods can transform macroscopic optical observations of tissues from a crude qualitative tool to an accurate three-dimensional imaging technique. This is important for capitalizing on the advantages of fluorescence and the bioluminescence methods: first, high molecular specificity; second, the use of nonionizing radiation that simplifies the operation and the chemical synthesis of reporter probes; third, the ability to use optical switches (molecular beacons) for achieving high sensitivity and specificity; fourth, optical probe stability because there is no intensity decay over time; and fifth, the potential for simultaneous investigations of multiple targets using spectral differentiation of probes.

These imaging principles can be applied to different biomedical research areas, including cancer, cardiovascular, immunologic/inflammatory and neurodegenerative diseases[5,10,11]. Important to these new developments is the accessibility of a larger number of sites and organs compared to the number that can be assessed using planar imaging. While small animal photonic tomography does not reach the resolution of optical microscopy, molecular activity is detected based on the high specificity of the optical probes employed (similarly to PET and SPECT), even if single cells and molecules are not explicitly resolved.

One other advantage of fluorescence tomography is that it can be combined with microscopy in a straightforward manner. Because it uses the same optical probe as fluorescence microscopy, a sample can first be visualized and quantified volumetrically *in vivo* as a function of time and then observed at high resolution with microscopy using excised samples or surgical intervention in the case of tissues that are not typically accessible by microscopy (that is, when samples are deeper or larger than ~400–700 µm).

The combination of modalities with complementing features offers an attractive future direction for study. Although optical tomography yields high molecular contrast versatility and specificity, photoacoustic imaging offers improved resolution to imaging light absorption. The combination of the two techniques could not only yield a straightforward superposition of optical and photoacoustic images, but also use PAT images as a priori information for constructing more accurate models for photon propagation in tissues, which will further mitigate the optical inversion problem. Other imaging modalities, such as CT, MRI or ultrasound, may also be used to register PAT images or fluorescence images onto high-resolution anatomical images, thereby improving the information content of the combined imaging approach.

Overall, these new technologies will continue to emerge and diversify, and new clinical applications will be identified; for example, in imaging human joints or the breast, in eye healthcare and in endoscopic applications, where appropriate photon models and limited angle projections would improve imaging performance. Currently, only a few sets of approaches and ideas about photonic imaging methodology have been explored. Light offers a plethora of contrast mechanisms and can be manipulated in several ways to further improve the performance and capability of these methods.

1. Massoud, T.F. & Gambhir, S.S. Molecular imaging in living subjects: seeing fundamental biological processes in a new light. *Genes Dev.* **17**, 545–580 (2003).
2. Blasberg, R.G. *In vivo* molecular-genetic imaging: multi-modality nuclear and optical combinations. *Nucl. Med. Biol.* **30**, 879–888 (2003).
3. Budinger, T.F., Benaron, D.A. & Koretsky, A.P. Imaging transgenic animals. *Annu. Rev. Biomed. Eng.* **1**, 611–648 (1999).
4. Contag, C.H. & Bachmann, M.H. Advances in *in vivo* bioluminescence imaging of gene expression. *Annu. Rev. Biomed. Eng.* **4**, 235–260 (2002).
5. Piwnica-Worms, D., Schuster, D.P. & Garbow, J.R. Molecular imaging of host-pathogen interactions in intact small animals. *Cell. Microbiol.* **6**, 319–331 (2004).
6. Weissleder, R. Scaling down imaging: molecular mapping of cancer in mice. *Nat. Rev. Cancer* **2**, 11–18 (2002).
7. Hoffman, R. Green fluorescent protein imaging of tumour growth, metastasis, and angiogenesis in mouse models. *Lancet Oncol.* **3**, 546–556 (2002).
8. Bornhop, D.J., Contag, C.H., Licha, K. & Murphy, C.J. Advance in contrast agents, reporters, and detection. *J. Biomed. Opt.* **6**, 106–110 (2001).
9. Tung, C., Mahmood, U., Bredow, S. & Weissleder, R. *In vivo* imaging of proteolytic enzyme activity using a novel molecular reporter. *Cancer Res.* **60**, 4953–4958 (2000).
10. Herschman, H.R. Molecular imaging: looking at problems, seeing solutions. *Science* **302**, 605–608 (2003).
11. Weissleder, R. & Ntziachristos, V. Shedding light onto live molecular targets. *Nat. Med.* **9**, 123–128 (2003).
12. Reynolds, J.S. *et al.* Imaging of spontaneous canine mammary tumors using fluorescent contrast agents. *Photochem. Photobiol.* **70**, 87–94 (1999).
13. Mahmood, U., Tung, C., Bogdanov, A. & Weissleder, R. Near infrared optical imaging system to detect tumor protease activity. *Radiology* **213**, 866–870 (1999).
14. Yang, M. *et al.* Whole-body optical imaging of green fluorescent protein-expressing tumors and metastases. Proc. *Natl. Acad. Sci. USA* **97**, 1206–1211 (2000).
15. Contag, C.H. & Ross, B.D. It's not just about anatomy: *in vivo* bioluminescence imaging as an eyepiece into biology. *J. Magn. Reson. Imaging* **16**, 378–387 (2002).
16. Farkas, D.L. *et al.* Non-invasive image acquisition and advanced processing in optical bioimaging. *Comput. Med. Imaging Graph.* **22**, 89–102 (1998).
17. Gao, X., Cui, Y., Levenson, R.M., Chung, L.W.K. & Nie, S. *In vivo* cancer targeting and imaging with semiconductor quantum dots. *Nat. Biotechnol.* **22**, 969–976 (2004).
18. Arridge, S.R., Schweiger, M., Hiraoka, M. & Delpy, D.T.A. *Finite-Element Approach For Modeling Photon Transport In Tissue. Med. Phys.* **20**, 299–309 (1993).
19. Graber, H.L. & Barbour, R.L. High-resolution near-infrared (nir) imaging of dense scattering media by diffusion tomography. *FASEB J.* **7**, A720–A720 (1993).
20. Schotland, J.C. & Leigh, J.S. Photon diffusion imaging. *FASEB J.* **6**, A446–A446 (1992).
21. Yodh, A.G. & Chance, B. Spectroscopy and imaging with diffusing light. *Phys. Today* **48**, 34–40 (1995).
22. Chance, B. Optical Method. *Annu. Rev. Biophys. Biophys. Chem.* **20**, 1–28 (1991).
23. Jobsis, F.F. Noninvasive, infrared monitoring of cerebral and myocardial oxygen sufficiency and circulatory parameters. *Science* **198**, 1264–1267 (1977).
24. Patterson, M.S., Chance, B. & Wilson, B.C. Time resolved reflectance and transmittance for the noninvasive measurement of tissue optical-properties. *Appl. Opt.* **28**, 2331–2336 (1989).
25. Graves, E., Ripoll, J., Weissleder, R. & Ntziachristos, V.A. Sub-millimeter resolution fluorescence molecular imaging system for small animal imaging. *Med. Phys.* **30**, 901–911 (2003).
26. Alfano, R.R. *et al.* Time-resolved and nonlinear optical imaging for medical applications. *Ann. NY Acad. Sci.* **838**, 14–28 (1998).
27. Sevick, E.M., Chance, B., Leigh, J., Nioka, S. & Maris, M. Quantitation of time-resolved and frequency-resolved optical-spectra for the determination of tissue oxygenation. *Anal. Biochem.* **195**, 330–351 (1991).
28. Cai, W. *et al.* Optical tomographic image reconstruction from ultrafast time-sliced transmission measurements. *Appl. Opt.* **38**, 4237–4246 (1999).
29. Chen, K., Perelman, L.T., Zhang, Q.G., Dasari, R.R. & Feld, M.S. Optical computed tomography in a turbid medium using early arriving photons. *J. Biomed. Opt.* **5**, 144–154 (2000).
30. Turner, G., Zacharakis, I., Soubret, A. & Ntziachristos, V. Complete angle projection diffuse optical tomography using early photons. *Optics Letters* **30**, 409–411 (2005).
31. Boas, D.A., Oleary, M.A., Chance, B. & Yodh, A.G. Scattering of diffuse photon density waves by spherical inhomogeneities within turbid media - analytic solution and applications. *Proc. Natl. Acad. Sci. USA* **91**, 4887–4891 (1994).
32. Godavarty, A. *et al.* Fluorescence-enhanced optical imaging in large tissue volumes using a gain-modulated ICCD camera. *Phys. Med. Biol.* **48**, 1701–1720 (2003).

33. Boas, D.A. *et al.* Imaging the body with diffuse optical tomography. *IEEE Signal Process. Mag.* **18**, 57–75 (2001).
34. Ripoll, J., Schultz, R. & Ntziachristos, V. Free-space propagation of diffuse light: Theory and Experiments. *Phys. Rev. Lett.* **91**, 103901–103904 (2003).
35. Schultz, R., Ripoll, J. & Ntziachristos, V. Experimental fluorescence tomography of arbitrarily shaped diffuse objects using non-contact measurements. *Opt. Lett.* **28**, 1701–1703 (2003).
36. Schultz, R., Ripoll, J. & Ntziachristos, V. Fluorescence tomography of tissues with non-contact measurements. *IEEE Med. Imag.* **23**, 492–500 (2004).
37. Chang, J., Graber, H.L. & Barbour, R.L. Imaging of fluorescence in highly scattering media. *IEEE Trans. Biomed. Eng.* **44**, 810–822 (1997).
38. Eppstein, M.J., Hawrysz, D.J., Godavarty, A. & Sevick-Muraca, E.M. Three-dimensional, Bayesian image reconstruction from sparse and noisy data sets: near-infrared fluorescence tomography. *Proc. Natl. Acad. Sci. USA* **99**, 9619–9624 (2002).
39. Jiang, H.B. Frequency-domain fluorescent diffusion tomography: a finite- element-based algorithm and simulations. *Appl. Opt.* **37**, 5337–5343 (1998).
40. Milstein, A.B. *et al.* Fluorescence optical diffusion tomography. *Appl. Opt.* **42**, 3081–3094 (2003).
41. Ntziachristos, V. & Weissleder, R. Experimental three-dimensional fluorescence reconstruction of diffuse media using a normalized Born approximation. *Opt. Lett.* **26**, 893–895 (2001).
42. Klose, A.D. & Hielscher, A.H. Fluorescence tomography with simulated data based on the equation of radiative transfer. *Opt. Lett.* **28**, 1019–1021 (2003).
43. Dehghani, H., Arridge, S.R., Schweiger, M. & Delpy, D.T. Optical tomography in the presence of void regions. *J. Opt. Soc. Am. A Opt. Image Sci. Vis.* **17**, 1659–1670 (2000).
44. Ntziachristos, V., Tung, C., Bremer, C. & Weissleder, R. Fluorescence-mediated tomography resolves protease activity *in vivo. Nat. Med.* **8**, 757–760 (2002).
45. Ripoll, J., Nieto-Vesperinas, M., Weissleder, R. & Ntziachristos, V. Fast analytical approximation for arbitrary geometries in diffuse optical tomography. *Opt. Lett.* **27**, 527–529 (2002).

46. Gu, X., Xu, Y. & Jiang, H. Mesh-based enhancement schemes in diffuse optical tomography. *Med. Phys.* **30**, 861–869 (2003).
47. Ye, J.C., Bouman, C.A., Webb, K.J. & Millane, R.P. Nonlinear multigrid algorithms for Bayesian optical diffusion tomography. *IEEE Trans. Image Process.* **10**, 909–922 (2001).
48. Vernooy, J., Dentener, M., van Suylen, R., Buurman, W. & Wouters, E. Long-term intratracheal lipopolysaccharide exposure in mice results in chronic lung inflammation and persistent pathology. *Am. J. Respir. Cell Mol. Biol.* **26**, 152–159 (2002).
49. Lautwein, A. *et al.* Inflammatory stimuli recruit cathepsin activity to late endosomal compartments in human dendritic cells. *Eur. J. Immunol.* **32**, 3348–3357 (2002).
50. Prin-Mathieu, C. *et al.* Enzymatic activities of bovine peripheral blood leukocytes and milk polymorphonuclear neutrophils during intramammary inflammation caused by lipopolysaccharide. Clin. Diagn. *Lab. Immunol.* **9**, 812–817 (2002).
51. Weissleder, R., Tung, C.H., Mahmood, U. & Bogdanov, A. *In vivo* imaging of tumors with protease-activated near-infrared fluorescent probes. *Nat. Biotechnol.* **17**, 375–378 (1999).
52. Ntziachristos, V. *et al.* Visualization of anti-tumor treatment by means of fluorescence molecular tomography using an annexin V - Cy5.5 conjugate. *Proc. Natl. Acad. Sci. USA* **101**, 12294–12299 (2004).
53. Wang, G., Li, Y. & Jiang, M. Uniqueness theorems in bioluminescence tomography. *Med. Phys.* **31**, 2289–2299 (2004).
54. Gu, X., Zhang, Q., Larcom, L. & Jiang, H.B. Three-dimensional bioluminescence tomography with model-based reconstruction. *Opt. Express* **12**, 3996–4000 (2004).
55. Hoelen, C.G.A. & de Mul, F.F.M. Image reconstruction for photoacoustic scanning of tissue structures. *Appl. Opt.* **39**, 5872–5883 (2000).
56. Wang, X. *et al.* Noninvasive photoacoustic angiography of animal brains *in vivo* with near-infrared light and an optical contrast agent. *Opt. Lett.* **29**, 730–732 (2004).
57. Wang, X. *et al.* Noninvasive laser-induced photoacoustic tomography for structural and functional *in vivo* imaging of the brain. *Nat. Biotechnol.* **21**, 803–806 (2003).
58. Karabutov, A.A., Savateeva, E.V. & Oraevsky, A.A. Optoacoustic tomography: new modality of laser diagnostic systems. *Laser Phys.* **13**, 711–723 (2003).